Processes **2013**, *1*, 30-48; doi:10.3390/pr1020030

OPEN ACCESS

processes

ISSN 2227-9717

www.mdpi.com/journal/processes

Article

Density and Viscosity Measurement of Diesel Fuels at Combined High Pressure and Elevated Temperature

Carl Schaschke [1,*], Isobel Fletcher [1] and Norman Glen [2]

[1] Department of Chemical and Process Engineering, University of Strathclyde, Glasgow G1 1XJ, UK; E-Mail: isobel.fletcher@strath.ac.uk

[2] TUV NEL Ltd., East Kilbride, Glasgow, G75 0QF, UK; E-Mail: nglen@tuvnel.com

***** Author to whom correspondence should be addressed; E-Mail: carl.schaschke@strath.ac.uk; Tel.: +44-0-141-548-2371.

Received: 20 May 2013; in revised form: 24 June 2013 / Accepted: 2 July 2013 / Published: 19 July 2013

Abstract: We report the measurement of the viscosity and density of various diesel fuels, obtained from British refineries, at elevated pressures up to 500 MPa and temperatures in the range 298 K to 373 K. The measurement and prediction procedures of fluid properties under high pressure conditions is of increasing interest in many processes and systems including enhanced oil recovery, automotive engine fuel injection, braking, and hydraulic systems. Accurate data and understanding of the fluid characteristic in terms of pressure, volume and temperature is required particularly where the fluid is composed of a complex mixture or blend of aliphatic or aromatic hydrocarbons. In this study, high pressure viscosity data was obtained using a thermostatically-controlled falling sinker-type high pressure viscometer to provide reproducible and reliable viscosity data based on terminal velocity sinker fall times. This was supported with density measurements using a micro-pVT device. Both high-pressure devices were additionally capable of illustrating the freezing points of the hydrocarbon mixtures. This work has, thus, provided data that can extend the application of mixtures of commercially available fuels and to test the validity of available predictive density and viscosity models. This included a Tait-style equation for fluid compressibility prediction. For complex diesel fuel compositions, which have many unidentified components, the approach illustrates the need to apply appropriate correlations, which require accurate knowledge or prediction of thermodynamic properties.

Keywords: high pressure; diesel fuel; falling sinker viscometer; viscosity measurement

---

Nomenclature

a	attraction parameter, $m^6 \cdot mol^{-2}$
A	viscometer constant, mPa^{-1}
b	repulsion parameter, $m^3 \cdot mol^{-1}$
b_0, b_1, b_2	constants used in the Tait equation
B	constant used in Tait equation (Table 2), MPa
C	constant used in Tait equation (-)
g	gravitational acceleration, $m \cdot s^{-2}$
k_0, k_1, k_2	constant used in Tait equation (Table 2), MPa
L_S	length of sinker wall, m
L_T	length of tube between detection coils, m
m	sinker mass, kg
M	constant used in the Tait equation
p	pressure, MPa
p_0	ambient pressure, MPa
p_C	critical pressure, MPa
Re_m	modified Reynolds number, (-)
r_1	radius of sinker, m
r_2	inner radius of tube, m
R	universal gas constant, $kg \cdot mol^{-1} \cdot K^{-1}$
R^2	statistical correlation coefficient (-)
T	temperature, K
T_0	ambient temperature, K
T_C	critical temperature, K
t	sinker fall time, s
v_0	constant used in the Tait equation
v_S	terminal velocity of sinker, $m \cdot s^{-1}$
V	volume $mol \cdot m^{-3}$
V_C	critical volume ($mol \cdot m^{-3}$)
Z	compressibility factor (-)
$Z^{(o)}$, $Z^{(r)}$	compressibility factors of the simple and reference fluid

Greek symbols

α	thermal expansion coefficient, K^{-1}
β	pressure compression factor, MPa^{-1}
η	viscosity, mPa·s
ρ	liquid density, $kg \cdot m^{-3}$
ρ_{liq}	density of the liquid, $kg \cdot m^{-3}$
ρ_S	sinker density, $kg \cdot m^{-3}$
ω, $\omega^{(r)}$	acentric factors of the fluid and reference fluid

1. Introduction

The demand for transport, together with the increasing scarcity of world fuel resources, has been responsible for many of the advances in crude oil recovery, fuel development, and the internal combustion engine. Depleted oil reservoirs are increasingly being revisited with more sophisticated ways of recovering the remaining oil deep below ground level. Above land, developments over the past century have led to modern domestic automobiles and heavy goods vehicle units bearing little resemblance to the noisy, polluting, low power, and efficiency engines of the early pioneering models. The diesel engine, in particular, originally developed by Dr Rudolph Diesel at the end of the nineteenth century, has been completely revolutionized in recent times. The development of diesel engine technology has, to a large extent, been driven by legislation and the public demand for lower emissions of noise, particulates, and gas emissions including carbon monoxide, carbon dioxide, and the oxides of sulphur and nitrogen.

Unlike the early pioneering models, modern automotive diesel engines now operate using a high-pressure common rail system. This involves injecting fuel into the cylinders at very high pressure. The rapid atomization of the fuel with thorough mixing with air and compression ensures rapid and complete combustion. The result is high power efficiency, minimum noise, and low particulate emissions. This has consequently either reduced or eliminated the requirement for costly NOx after-treatment devices [1]. Within the European Union, such engines are also expected to start up and operate within a range of fuel compositions available from country to country, produced and available season to season and across a wide range of ambient and sub-ambient temperatures.

The common rail form of injection system has been successfully developed to meet the stringent requirements governing emissions of all types of diesel engines. This involves a single high-pressure fuel pump that feeds the fuel to a manifold (or common rail) from which the fuel is fed to the fuel injectors of each cylinder in the diesel engine. High-pressure injector nozzles to the engine cylinder are used provide a more complete combustion and reduction of soot emissions and noise levels and thus meet necessary legislative requirements [2].

The effective design of a fuel injection system requires the understanding of the thermophysical properties of the fuels over the range of conditions experienced by the common rail where pressure may be as high as 200 MPa. Leakage from the system is an important aspect of the design in which clearances must be sufficiently tight to prevent gross displacement of liquid fuel. However, there is a requirement for some free movement of moving parts. To assess the leakage rate, it is necessary to have an accurate estimate of the viscosity and density of the fuel and the flow behavior with respect to temperature and pressure. During leakage, pressure-volume energy is converted to thermal energy, raising the temperature of the fuel thereby affecting both the density and viscosity. An accurate measurement of the physical properties of viscosity and density of fuels is therefore essential to minimize errors in the design of diesel engines. Such knowledge is additionally essential in the accurate measurement of fuels such as crude oil at conditions experienced at source since crude oil is increasingly being sourced at greater depths, and thus higher pressures. It is essential to possess accurate estimates of the properties of a given crude composition with respect to pressure for fiscal flow accountancy purposes. High temperatures and extreme pressures are also encountered braking and hydraulic systems. The need for knowledge and understanding of the characteristics of complex

fluids in terms of pressure, volume, and temperature is essential if designs are to be safe, reliable, economic, and efficient.

For the common rail system, both density and viscosity of the diesel fuels can vary significantly under high pressure and temperature. There may also be a change of phase with potential blockage of narrow pipes and tubes. Equally, low ambient temperature diesel waxes can also cause blockage, which is a major issue particularly in the colder climes. Understanding of the behavior of these hydrocarbon fuels is therefore crucial [3]. While there are reports on the measurement and prediction of diesel properties at ambient or high temperature conditions, comparatively little work has been reported at high pressure and temperature [4,5]. Temperature effects on the dynamic viscosity and density of hydrocarbon and petroleum distillation cuts at high pressure are well known as is the phenomenon of pressure-freezing [6]. Fortunately, high temperatures and pressures are unlikely to affect the performance of the engine due to the time to reach equilibrium in running engines, particularly at the point of starting an engine from ambient temperatures. While there is a growing body of information concerning the variations of viscosity of substances with both temperature and pressure, we have, in this work, examined the combined effect of high pressure typically used in common rail engines and above at ambient and temperatures of up to 373K in terms of density prediction and viscosity measurement for a number of mineral diesel fuels taken directly from two British petrochemical refineries with and without additives.

2. Experimental Section

The (summer) diesel fuels examined in this work were obtained directly from two British refineries. These were

Fuel 1: Refinery 1 with no performance or handling additives.

Fuel 2: Refinery 1 with both handling and performance additives.

Fuel 3: Refinery 2 with both handling and performance additives.

Fuel 4: Refinery 2 with 5% rape methyl ester.

Fuel 5: A commercially available retail fuel.

2.1. High-Pressure Viscometer

The viscosity of the fuels was measured using a falling sinker high-pressure viscometer. This type of viscometer, designed and constructed by the National Engineering Laboratory consists of a vertical tube through which the sinker falls at terminal velocity, and has been previously used to measure the viscosity of both pure liquids and complex mixtures [7]. Both the tube and sinker were fabricated from a single piece of the same material (either non-magnetic En 58J stainless steel or titanium; for this work titanium was used), thereby minimizing compressibility and thermal expansion effects. The viscometer design is based on a falling sinker in which gravity is used to provide the applied force. Viscosity measurements are determined from the time taken for a cylindrical sinker to descend down a vertical tube containing the sample liquid. The entire viscometer tube was contained within a high-pressure vessel rated to 1 GPa. Having a hemispherical nose, and being self-centering, the descent of the sinker was detected by way of electrical signal induced by a ferrite core embedded into the sinker as it passed copper coils surrounding the tube. A change in inductance as the ferrite core of the

sinker passed each coil was transmitted through a bridge circuit and amplified for capture on a PC and recorded as peaks. The time taken to pass two coils, a given distance apart, and the dimensions of the viscometer and sinker were sufficient to determine the viscosity of the liquid with an appropriate calibration.

Figure 1. Falling body viscometer.

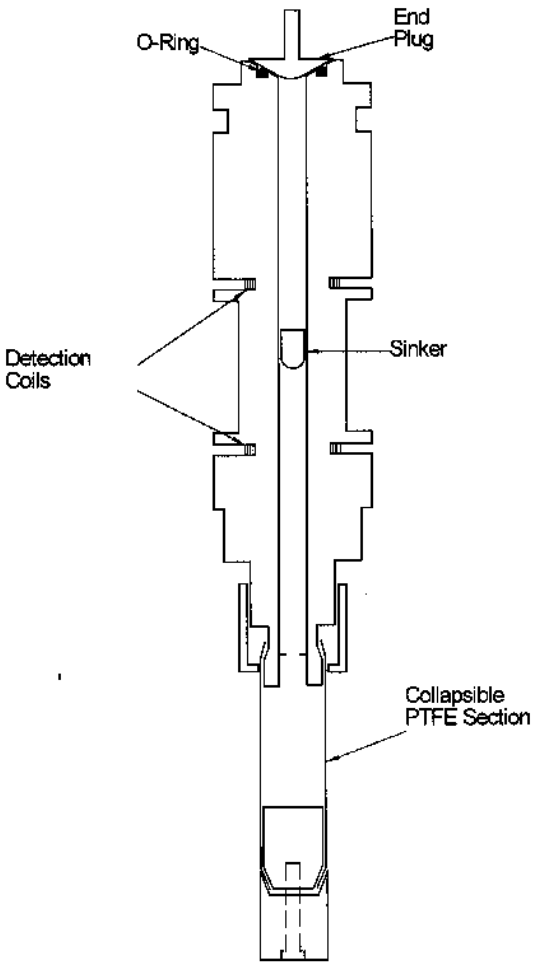

The viscometer assembly, shown in Figure 1, was approximately 23 cm in length, with an external diameter of 2.4 cm and an internal diameter of 7.645 mm. The sinker had a diameter of 7.420 mm with a small cylinder of ferrite embedded within the core. The sinker dimensions are significant in that the sinker is designed to be self-centering allowing it to descend through the center of the vertical tube containing the sample liquid. The viscosity was determined directly from the time taken for the sinker to descend at terminal velocity a fixed vertical distance of 14 mm between the two lacquered copper detection coils each with an approximate equal electrical resistance and wrapped around the outside of the tube. Terminal velocity was confirmed to have been reached, experimentally, far in advance of reaching the two coils. Both coils were connected in series and formed the active arm of a balanced bridge circuit. The three other arms of the bridge were remote from the viscometer and outside the vessel. The electrical connections passed out of the vessel through a ceramic seal. The out-of-balance electrical signal from the bridge was amplified and passed through an AC and DC converter for data-logging on a PC. As the sinker passed the detection coils, the DC signal increased to a maximum

at the point where the ferrite core of the sinker was positioned at the center of the coil. In this way, it was possible to have a peak corresponding to the sinker passing each coil. The sinker fall-time was measured in milliseconds and the duration of the sinker fall between the coils was dependent on the viscosity, typically ranging between 6000 and 30,000 milliseconds.

The pressure within the viscometer was generated and transmitted by a two stage pressurizing system using a paraffin/Shell Tellus oil mixture as the hydraulic medium. Pressures up to 200 MPa were generated directly via an air-driven pump operating from a 7 bar airline. Higher pressures (up to a possible maximum of 500 MPa) were generated using a piston intensifier. The hydraulic pressure was transmitted to the sample fuels using a PTFE expansion sheath located at the bottom of the viscometer tube to allow for compression of the samples. A calibrated Kistler piezo-resistive pressure gauge type 4618A0 was used to measure the high pressure within the pressure vessel. Over the course of a fall time measurement, the pressure in the vessel was normally stable to within 0.2 MPa. The viscometer operated with the vertical descent of the sinker down the tube. To return the sinker to its original starting position between each measurement the entire pressure vessel was inverted.

From the time taken for the sinker to pass the two detection coils, the viscosity was able to be determined analytically from the free descent of the sinker under the influence of gravity based on the shear stress profile across the annular gap [8].

The equations of motion of a cylindrical body falling axially down a vertical circular tube with laminar flow have been previously given by Isdale [9]. For the sinker, which falls a defined distance between the two detected coils a distance L_T apart in time *t*, the viscosity is determined to be:

$$\eta = \frac{t\left(1 - \frac{\rho_{liq}}{\rho_S}\right)}{A(1 + 2\alpha(T - T_0)(1 - 2\beta(p - p_0)} \tag{1}$$

where A is based on the physical dimensions of the sinker and tube given by:

$$A = \frac{2\pi L_S L_T}{mg\left(\ln\left(\frac{r_2}{r_1}\right) - \frac{r_2^2 - r_1^2}{r_2^2 + r_1^2}\right)} \tag{2}$$

In practice, however, there is a discrepancy between the actual viscosity and determined viscosity due to vortex shedding from the tail of the sinker present, even at very low Reynolds numbers. This has been previously confirmed by both experiment and CFD analysis [8]. It is also known that fully developed laminar flow does not exist within the annulus.

Calibration data using iso-octane, hexadecane and S20 oil at temperatures from 298.14 to 373.17 K were obtained in triplicate and examined in relation to a modified Reynolds number (Re_m) within the annulus between the sinker and tube of the form:

$$\mathrm{Re}_m = \frac{2\rho_{liq} v_S r_1^2}{\eta(r_2 + r_1)} \tag{3}$$

The derivation of Re_m has been shown previously [10]. High viscosity fluids provide longer sinker fall times in which the fluid exhibits a lower Reynolds number. From the physical dimensions of the

sinker and using the properties of iso-octane, hexadecane and S20 oil, the calibration coefficients were determined for the various temperatures studied [11] (Table 1).

Table 1. Viscometer calibration.

Liquid	Temperature (K)	Fall time (s)	Re (-)	*A* (-)
Iso-octane	298.1	2.089	77.0	3.852
	323.2	1.618	126.7	3.941
	348.2	1.323	191.0	4.122
	373.2	1.171	258.1	4.550
Hexadecane	298.2	13.529	2.047	3.768
	323.2	8.026	5.618	3.734
	348.2	5.425	12.11	3.775
	373.1	3.913	22.72	3.783
S20 Oil	298.2	137.82	0.022	3.702
	323.2	50.448	0.161	3.731
	348.2	24.524	0.161	3.745
	373.1	14.265	1.943	3.755

Two correlations for A were found, one for low Reynolds numbers and another for higher Reynolds numbers:

$$\begin{aligned} A &= 03.645 + 0.0978\,\mathrm{Re}^{0.1} \qquad (0 < \mathrm{Re} < 25) \\ A &= 3.792 + 7.024\times10^{-7}\,\mathrm{Re}^{2.5} \quad (25 < \mathrm{Re} < 60) \end{aligned} \tag{4}$$

The temperature of the viscometer tube was thermostatically controlled; the entire pressure vessel containing the viscometer tube was immersed in 240 liters of oil with temperature generation and control provided by steel-sheathed, mineral-insulated heating coils. Five coils provided constant background heating for high temperature operation. In conjunction with a thermostatically-controlled coil, this enabled the oil to be set and maintained at any temperature between 298 K and 373 K. In addition, the oil tank containing the pressure vessel was insulated to reduce heat loss, with at least one hour allowed to reach equilibrium for each of the temperatures. The average temperature of the oil in the bath was measured using two calibrated 100 Ω platinum resistance thermometers. Over the course of a fall-time measurement the average temperature of the oil was normally stable to within 0.05 K. Previous work [9] had shown that this corresponds to temperature stability of 0.005 K in the viscometer, due to the thermal inertia of the pressure vessel. For this work, set point temperatures of 298 K, 323 K, 348 K, and 373 K were used.

At each temperature and pressure, a minimum of three fall-time measurements were made or until three consecutive measurements agreed to within 0.2% of the mean value. However, a full uncertainty analysis indicates that the uncertainty in viscosity at elevated temperature and pressure is 2.0% (at k = 2), primarily due to the contribution arising from the calibration process.

2.2. Density Determinations

The determination of accurate viscosity data using the high-pressure viscometer requires the availability of accurate liquid density data. Compressed liquid density at elevated pressure and

temperature can be measured with some certainty using experimental methods. Usually, in the absence of an accurate experimental procedure, density data are obtained using equations of state or various empirical formulae, often with a high degree of certainty [12,13]. In this case, equations of state, the Lee-Kesler and experimental procedures were used and compared.

Density data were determined experimentally with pressures also up to 500 MPa using a micro-PVT device at temperatures of 298 K, 323 K, 348 K, and 373 K. This device was based on a piston-in-bottle design and operated by means of translational-rotary displacement of a metal rod, which compressed the liquid sample at constant rate. The force exerted on the fluid was measured directly by a pressure sensor within the cell and the volume change determined from the displacement of the rod. Rotation of the rod minimized the friction between the rod and the seals. Pseudo-isothermal conditions were maintained during compression by using a low-speed of rotation and circulating water from a constant temperature water bath through a thermostatic jacket surrounding the high-pressure cell. The initial liquid volume was calculated from the reference position of the rod and the change in position of the rod from this reference position. The uncertainty of pressure measurement for the apparatus has been estimated to be better than 0.5 MPa over the 500 MPa range with an allowance being made for change in cell volume due to temperature and pressure [11].

In principle, the micro-PVT device can be used in an absolute mode but like the falling sinker viscometer, improved accuracy can be obtained by calibration, in this case with fluids of known density. For this work iso-octane was used as the calibration fluid and a correction function derived. A full uncertainty analysis indicates that the density at elevated temperature and pressure is within 0.2% (at $k = 2$).

To support the experimental density determinations, density determinations were obtained from well-known cubic equations of state of the form:

$$p = \frac{RT}{V-b} - \frac{a}{(V+k_1 b)(V+k_2 b)} \tag{5}$$

and using critical point data to determine a and b where:

$$\text{Van der Waals: } k_1 = 0,\ k_2 = 0,\ a = 3p_C V_C^2,\ b = \frac{V_C}{3} \tag{6}$$

$$\text{Redlich-Kwong: } k_1 = 0,\ k_2 = 1,\ a = 0.4275\frac{R^2 T_C^2}{p_C},\ b = 0.0866\frac{RT_C}{p_C} \tag{7}$$

$$\text{Peng-Robinson: } k_1 = 1,\ k_2 = 1,\ a = 0.4572\frac{R^2 T_C^2}{p_C},\ b = 0.0778\frac{RT_C}{p_C} \tag{8}$$

While the Peng-Robinson equation of state provides the best estimate for hydrocarbons an uncertainty of better than 1% should be considered in proportion to the uncertainty of fall-time measurement and consequent influence on viscosity estimation. For more accurate work, a versatile method for the prediction of dense fluid thermodynamic properties is that of Lee and Kesler [14]. Unlike other methods, this method uses published critical property and acentric factor data directly without the calculation of intermediary characteristic parameters. This uses a three corresponding

states principle to calculate the compressibility factor of the fluid of interest with respect to those of a simple fluid and a reference fluid defined by:

$$Z = Z^{(o)} + \frac{\omega}{\omega^{(r)}}\left(Z^{(r)} - Z^{(o)}\right) \tag{9}$$

$Z^{(o)}$ and $Z^{(r)}$ represent the compressibility factors of the simple and reference fluid, ω and $\omega^{(r)}$ are the acentric factors of the fluid of interest and the reference fluid. The Lee-Kesler equation, however, is an interpolation of the supposed straight-line relation between the acentric factor and compressibility with the special case of $\omega^{(o)} = 0$ as one of the reference points. For a more general case of the two fluids being chosen as the reference fluid, the interpolation equation is:

$$Z = Z^{(r_1)} + \left(\omega - \omega^{(r_1)}\right)\left(\frac{Z^{(r_2)} - Z^{(r_1)}}{\omega^{(r_2)} - \omega^{(r_1)}}\right) \tag{10}$$

As a method, it is desirable that the fluids used cover the range of acentric factors encountered in diesel fuel. A GC-FID analysis of several diesel fuels has shown that n-alkanes follow a normal distribution between C9 and C24, with C15 being the most abundant mass fraction. While straight chain n-alkanes between C10 and C19 individually constitute less than 1% of the total mass of diesel fuel mixture, the chain length of many of the components varies significantly [9]. As a consequence, iso-octane (2,4,4-trimethylpentane) and heptadecane were chosen as the reference fluids. Data were then fitted to a Tait-style equation to determine the compressibility factor as a function of both pressure and temperature of the form:

$$Z = \frac{p' v_0}{RT}\left(1 - C\log_{10}\left(\frac{B + p}{B + 0.1}\right)\right) \tag{11}$$

where B and C are the Tait coefficients for the fluid with C being a constant for each fluid and B a linear function temperature. v_o is expressed as a function of temperature as:

$$v_0 = \frac{M}{1000}\left(k_0 + k_1 T + k_2 T^2\right)^{-1} \tag{12}$$

where M is a constant and:

$$B = b_0 + b_1 T + b_2 T^2 \tag{13}$$

The constants are given in Table 2.

Table 2. Constants used in the Tait equation.

Fluid	$k_0 \times 10^{-3}$	$k_1 \times 10^{-6}$	$k_2 \times 10^{-9}$	b_0	b_1	$b_2 \times 10^{-3}$	C
iso-octane	1.3549	1.0667	4.6851	300.94	−1.1327	1.0926	0.207
heptadecane	1.1382	0.047394	1.878	316.76	−0.93033	0.69114	0.203

3. Results and Discussion

Density and viscosity measurements were made over a range of conditions for five different diesel fuels. The variation of viscosity and density with pressure for different temperatures are shown in Figures 2–11. The experimental viscosity and density correlations are presented in Tables 3 and 4.

Figure 2. Variation of viscosity for Fuel 1 with temperature. ♦ 298 K, ■ 323 K, ▲ 348 K, and X 373 K.

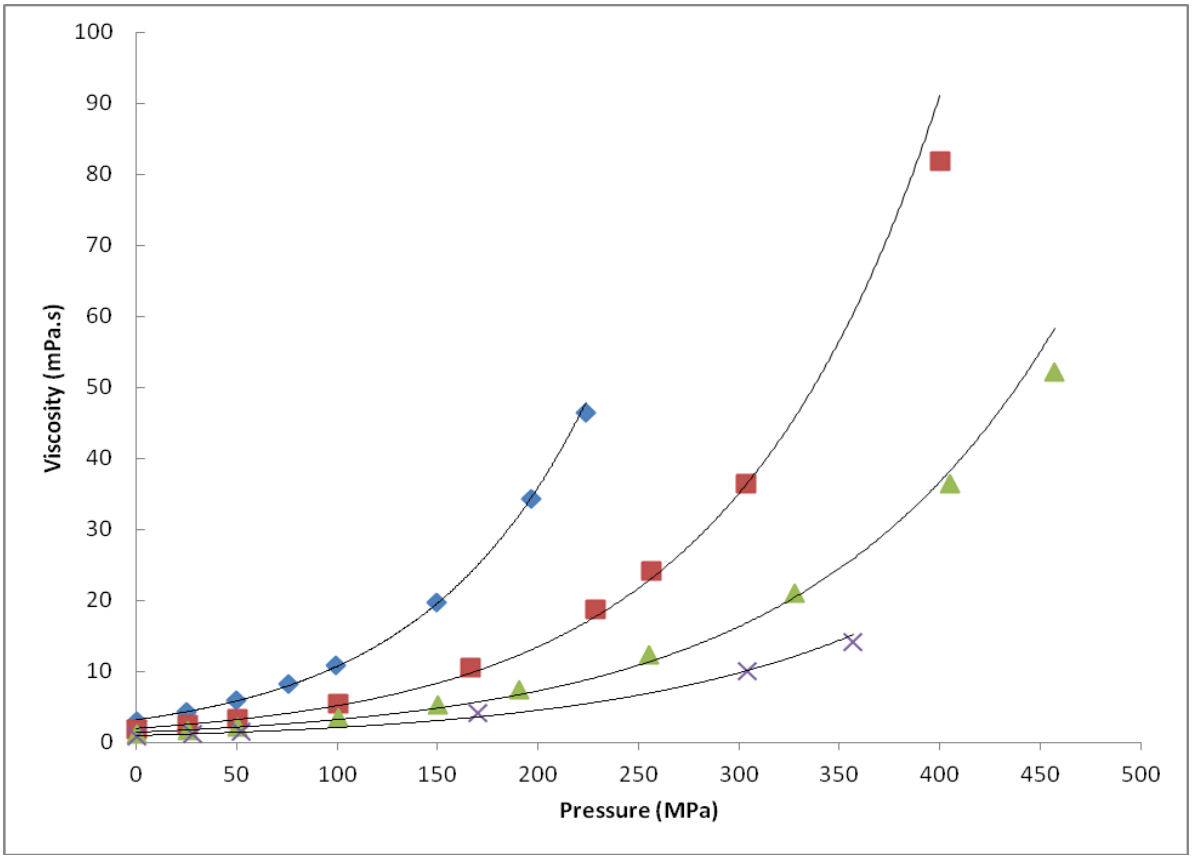

Figure 3. Variation of density for Fuel 1 with temperature. ♦ 298 K, ■ 323 K, ▲ 348 K, and X 373 K.

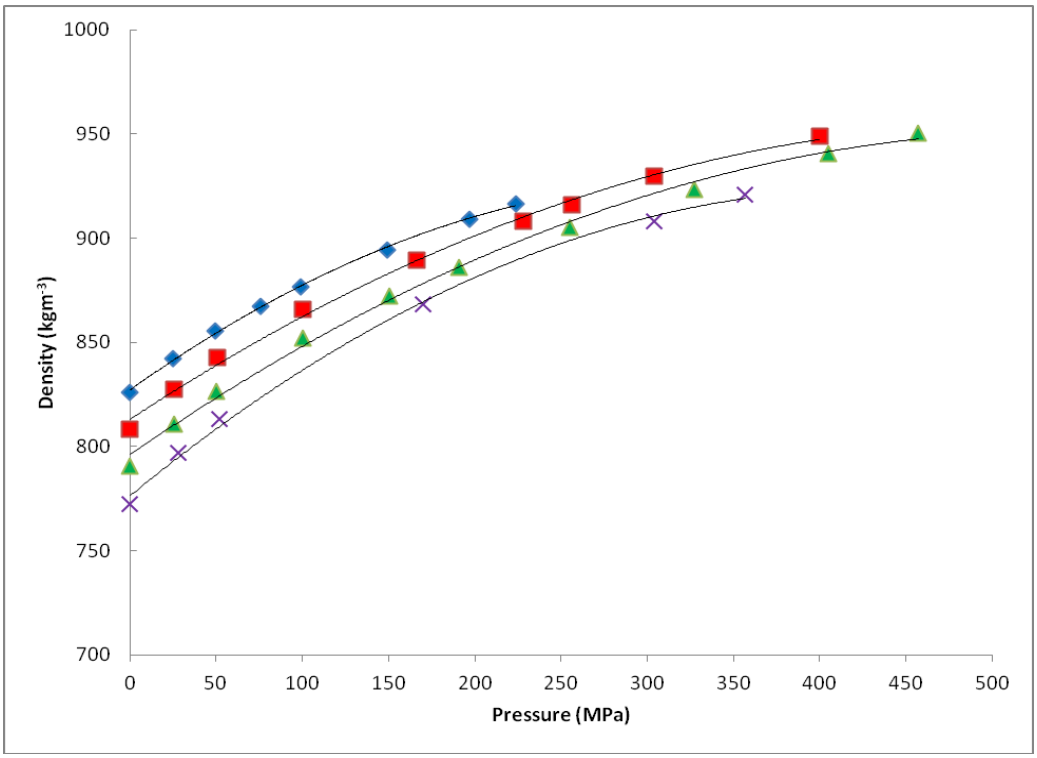

Figure 4. Variation of viscosity for Fuel 2 with temperature. ♦ 298 K, ■ 323 K, ▲ 348 K, and X 373 K.

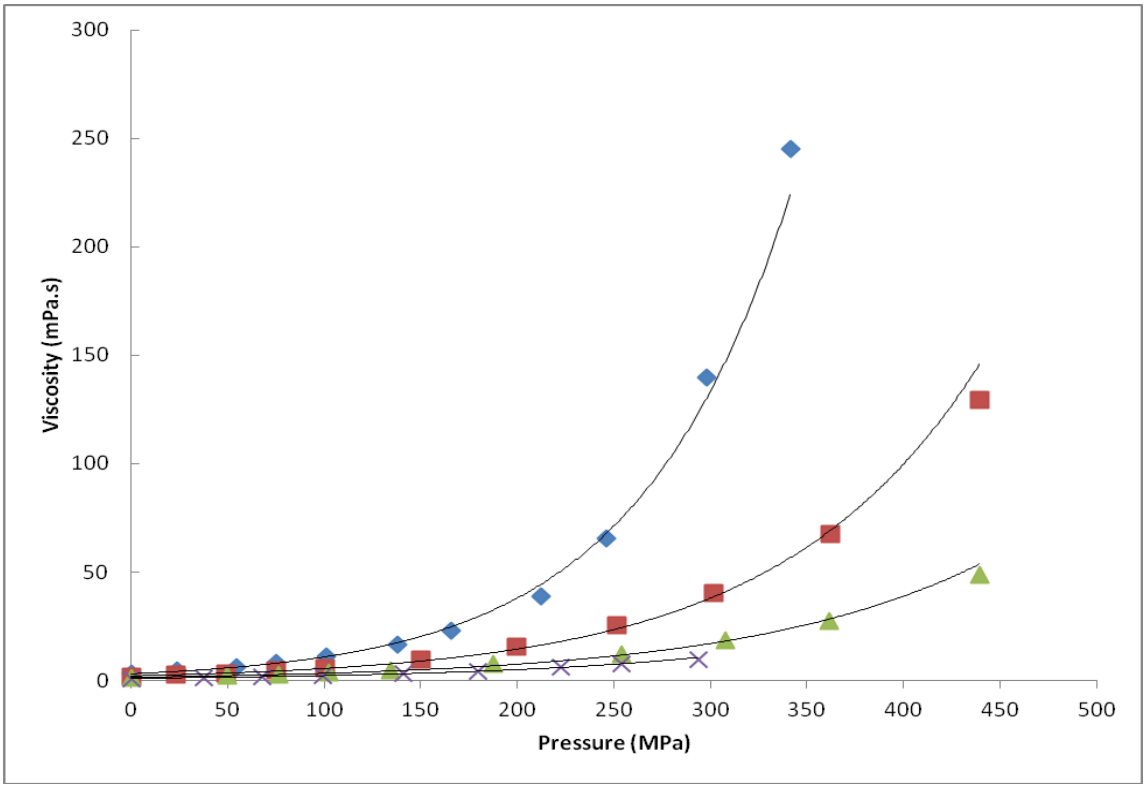

Figure 5. Variation of density for Fuel 2 with temperature. ♦ 298 K, ■ 323 K, ▲ 348 K, and X 373 K.

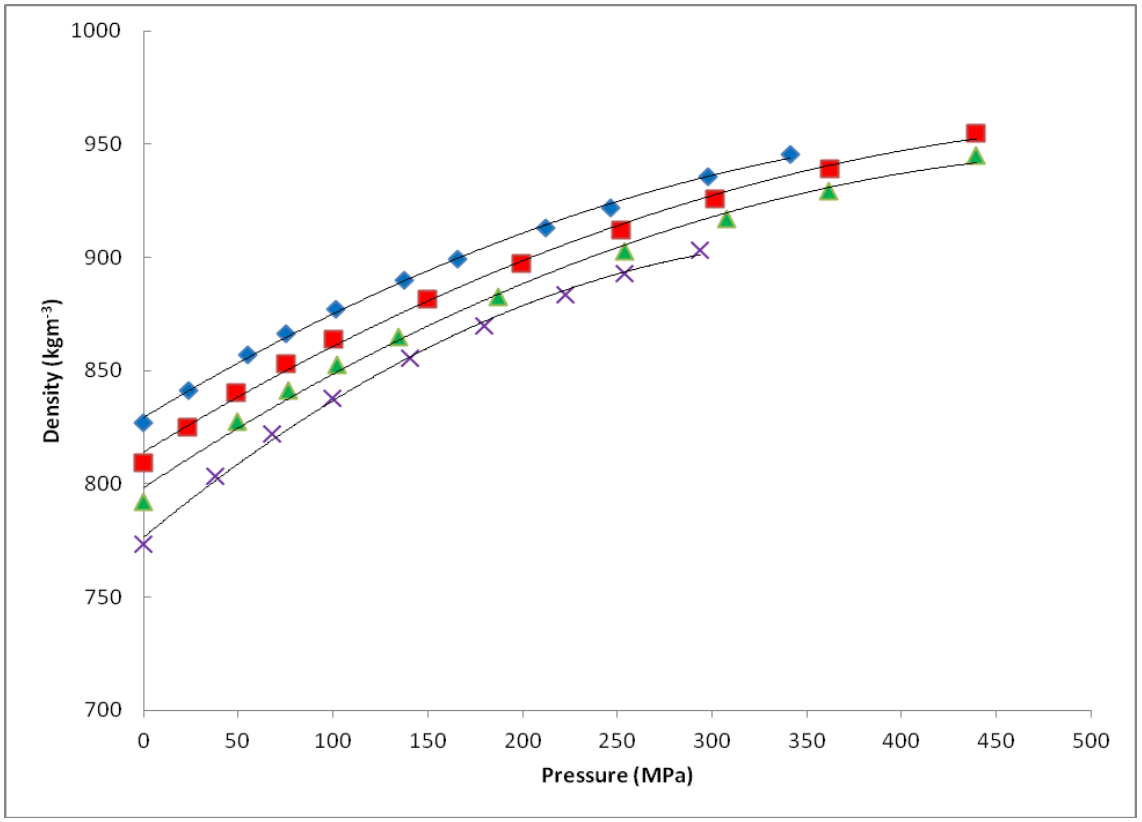

Figure 6. Variation of viscosity for Fuel 3 with temperature. ♦ 298 K, ■ 323 K, and ▲ 348 K.

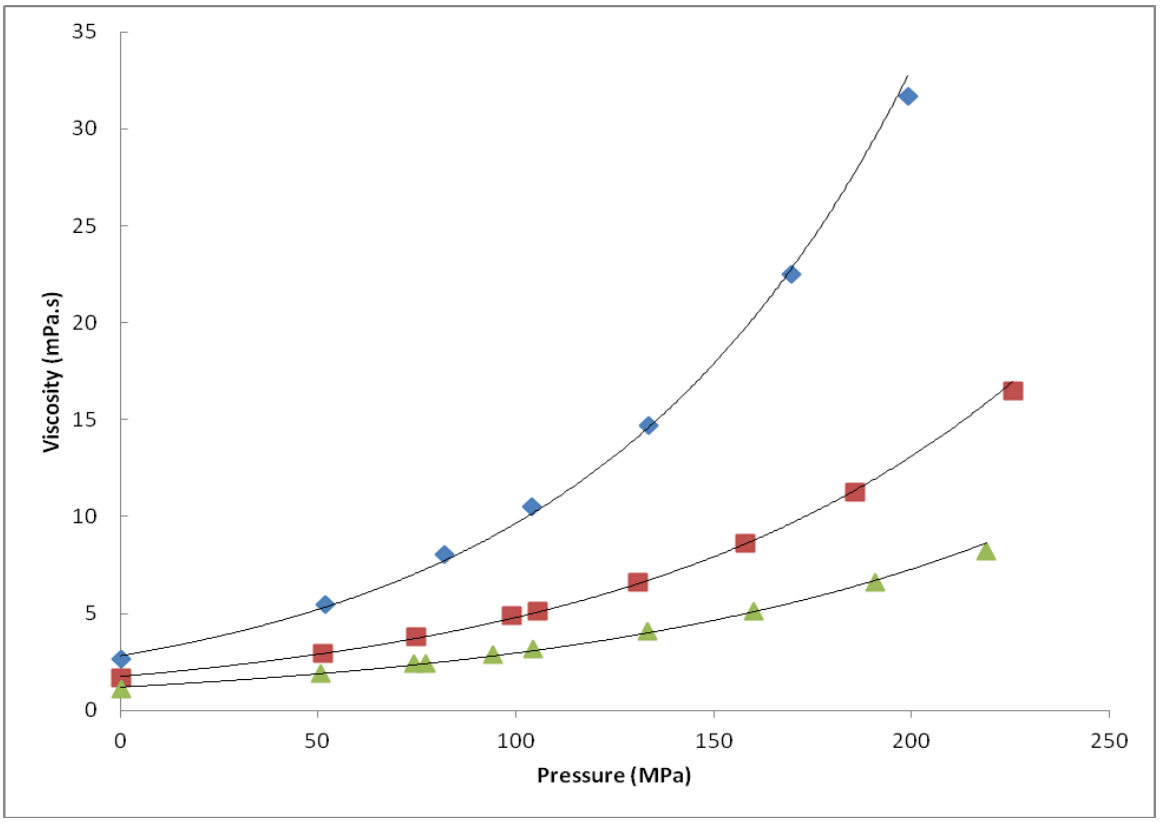

Figure 7. Variation of density for Fuel 3 with temperature. ♦ 298 K, ■ 323 K, and ▲ 348 K.

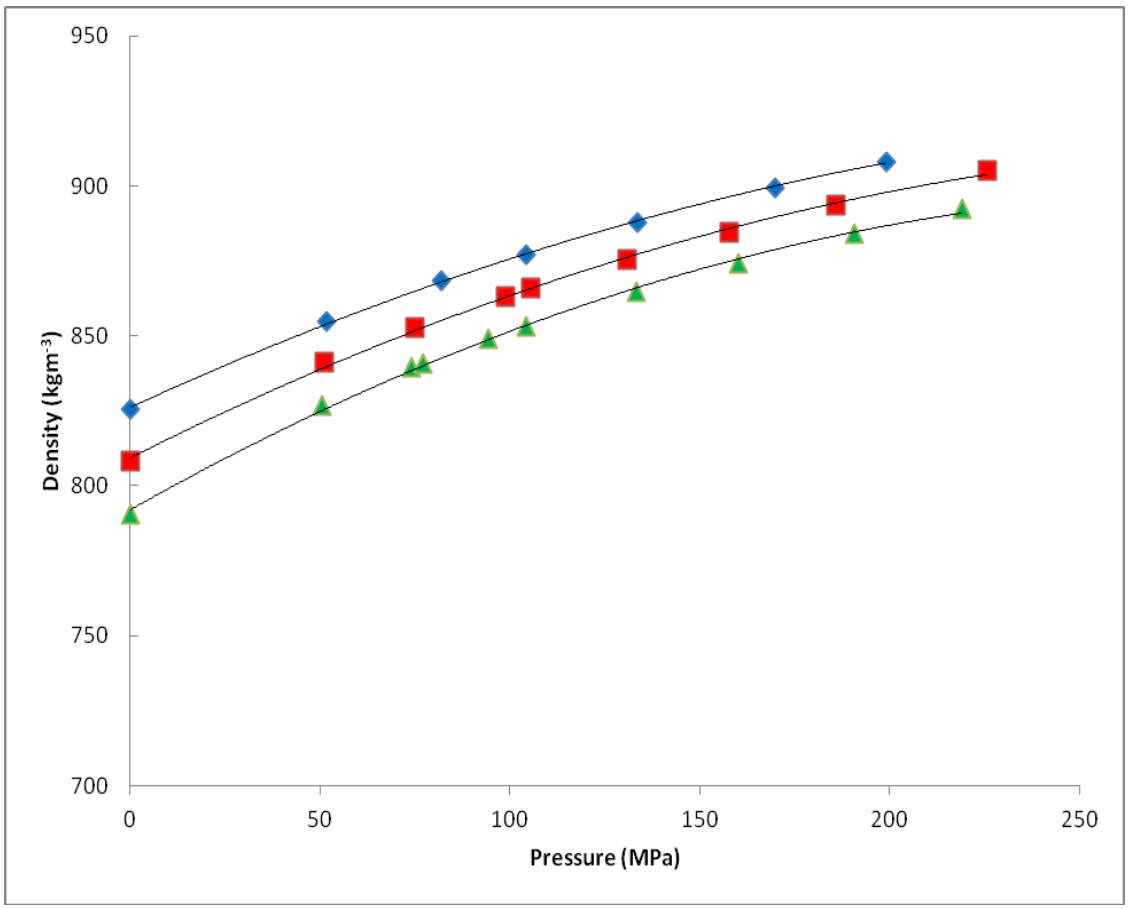

Figure 8. Variation of viscosity for Fuel 4 with temperature. ♦ 298 K, ■ 323 K, and ▲ 348 K.

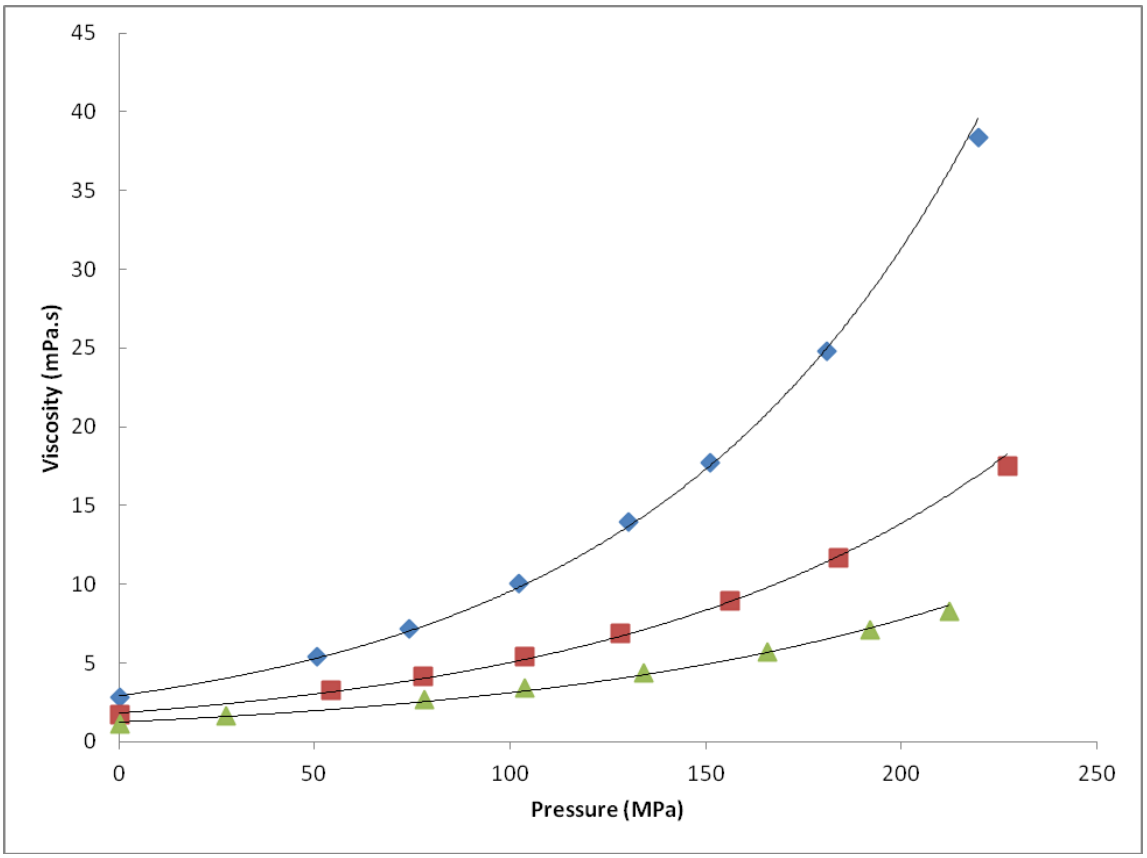

Figure 9. Variation of density for Fuel 4 with temperature. ♦ 298 K, ■ 323 K, and ▲ 348 K.

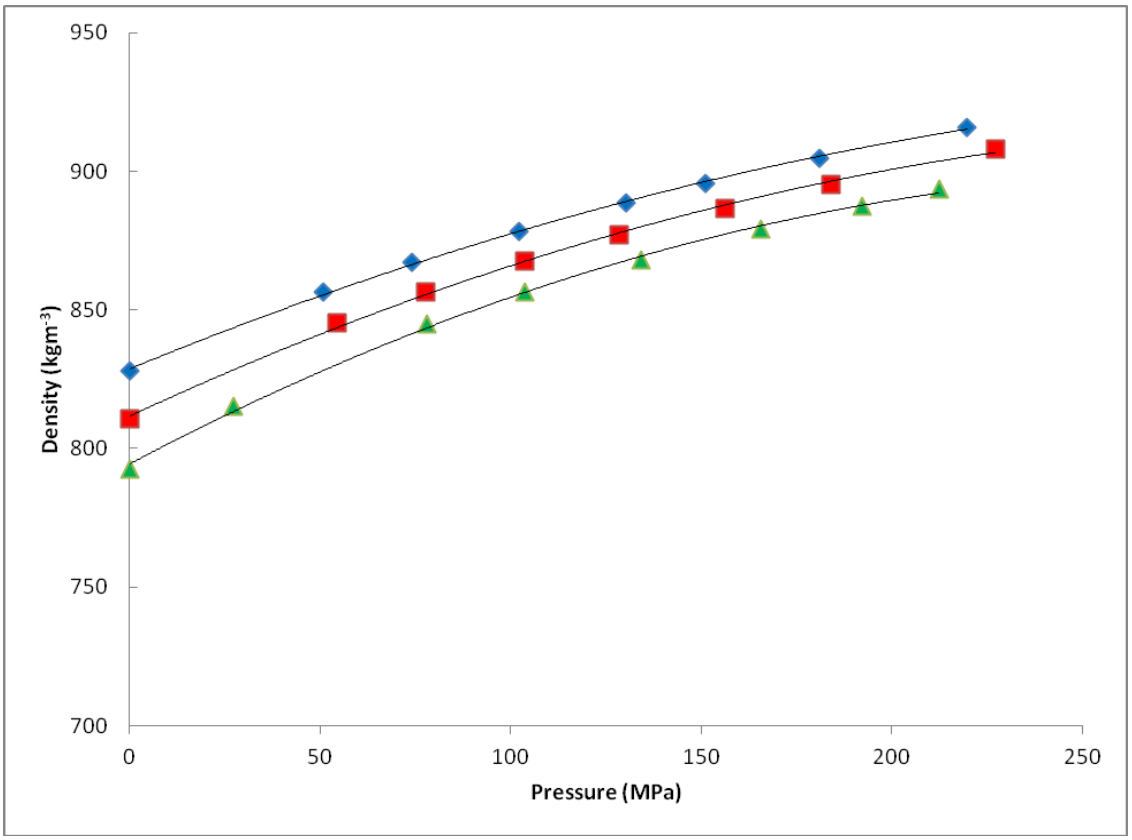

Figure 10. Variation of viscosity for Fuel 5 with temperature. ♦ 298 K, ■ 323 K, and ▲ 348 K.

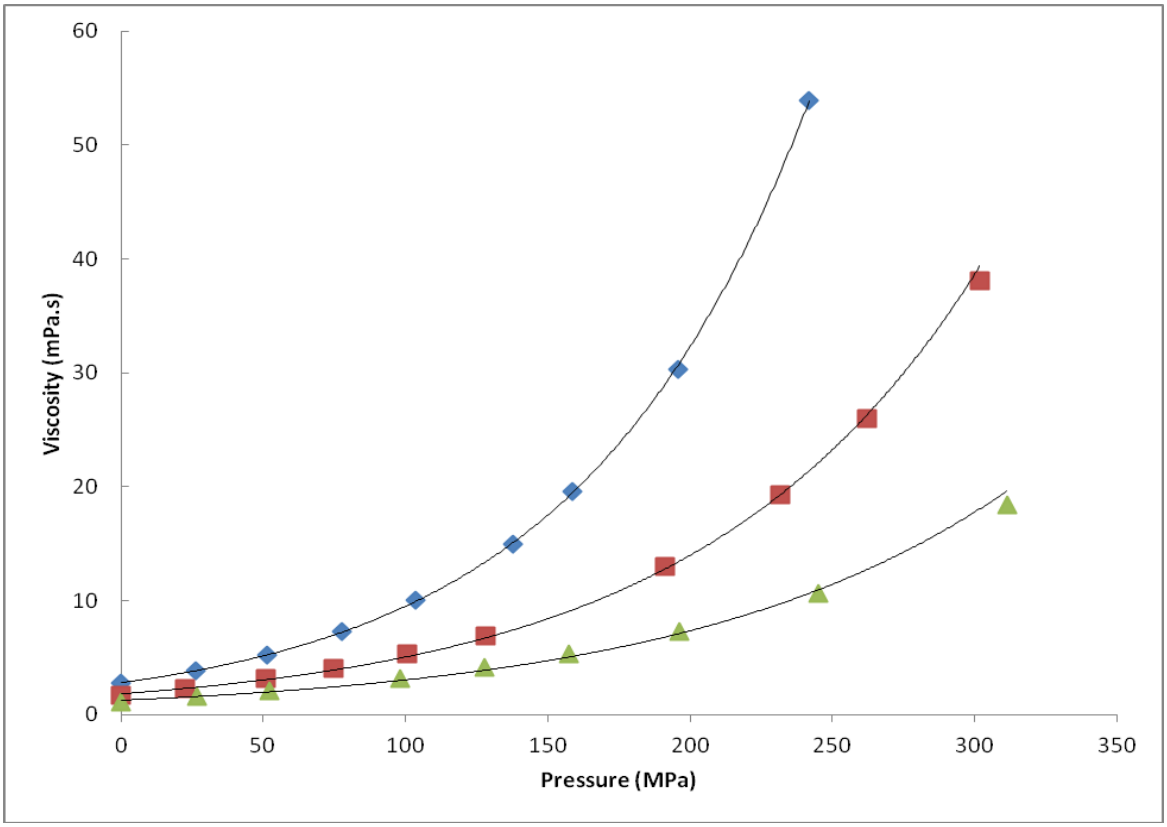

Figure 11. Variation of density for Fuel 5 with temperature. ♦ 298 K, ■ 323 K, and ▲ 348 K.

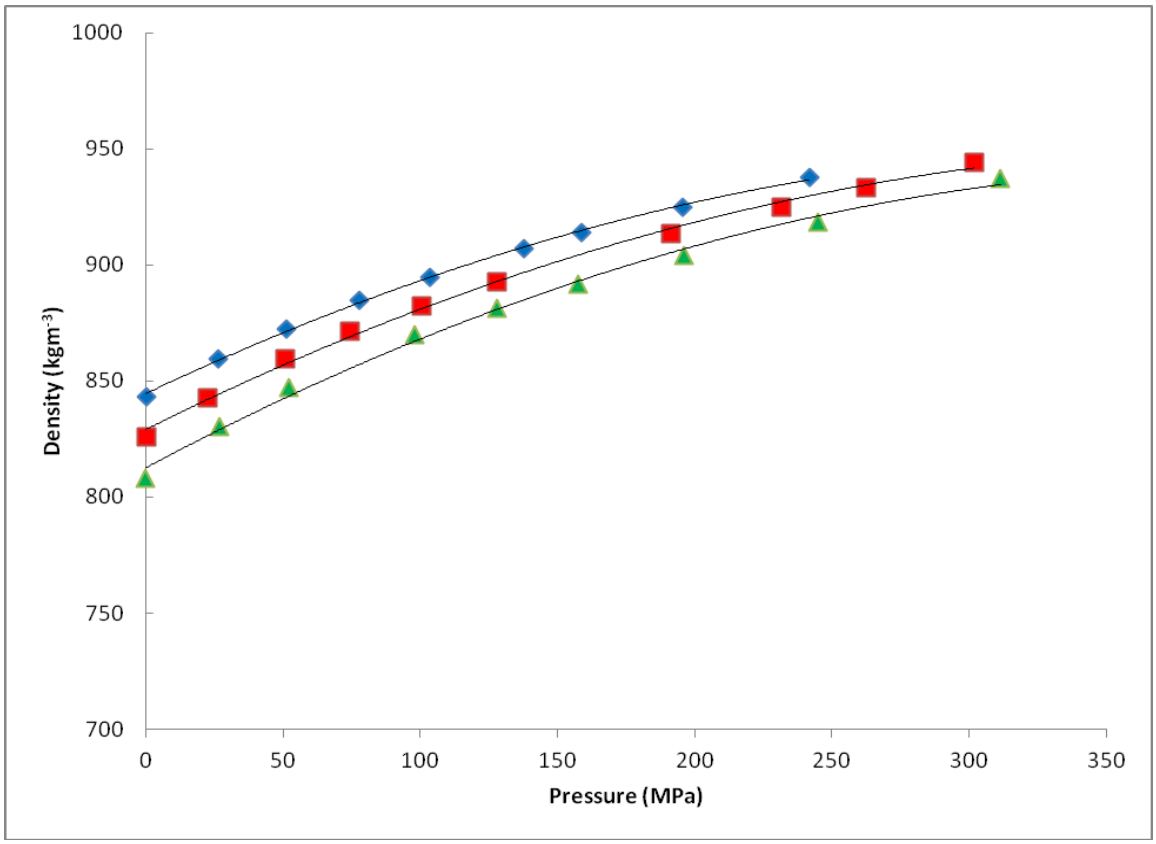

Table 3. Viscosity correlations with pressure for Fuels 1 to 5.

Fuel	Viscosity η (mPa.s)			
	298 K	323 K	348 K	373 K
1	$3.20e^{0121p}$	$1.99e^{0.0096p}$	$1.44e^{0.0081p}$	$0.972e^{0.0077p}$
2	$3.09e^{0.0126p}$	$2.10e^{0.0097p}$	$1.44e^{0.0082p}$	$0.987e^{0.0081p}$
3	$2.82e^{0.0123p}$	$1.75e^{0.0101p}$	$1.20e^{0.0090p}$	nd
4	$2.91e^{0.0119p}$	$1.82e^{0.9974p}$	$1.25e^{0.0090p}$	nd
5	$2.80e^{0.0122p}$	$1.83e^{0.0102p}$	$1.26e^{0.0088p}$	nd

Values of R^2 varied between 0.9935 and 1; nd: not determined.

Table 4. Density correlations with pressure for Fuels 1 to 5.

Fuel	Density ρ (kg·m^{-3})			
	298 K	323 K	348 K	373 K
1	$827 + 0.590p - 0.0009p^2$	$813 + 0.545p - 0.0005p^2$	$796 + 0.574p - 0.0005p^2$	$776 + 0.682p - 0.0008p^2$
2	$829 + 0.508p - 0.005p^2$	$814 + 0.513p - 0.0004p^2$	$798 + 0.553p - 0.0005p^2$	$798 + 0.553p - 0.0005p^2$
3	$826 + 0.582p - 0.0009p^2$	$809 + 0.638p - 0.0010p^2$	$809 + 0.638p - 0.0010p^2$	nd
4	$829 + 0.566p - 0.0008p^2$	$812 + 0.639p - 0.0010p^2$	$794 + 0.727p - 0.0013p^2$	nd
5	$845 + 0.561p - 0.0007p^2$	$829 + 0.590p - 0.0007p^2$	$813 + 0.632p - 0.0008p^2$	nd

R^2 for each of the above multiple regressions were between 0.995 and 0.999; nd: not determined.

In general terms, the variation of viscosity with pressure for each of the fuels was found to be logarithmic in nature and was conveniently correlated with the exponential barus equation of the form $p = ae^{bp}$ (Table 3). These correlations were found to fit up to the point that the sinker was unable to descend due to a change in phase as the result of blockage caused by the phase change of the larger hydrocarbon components. This pressure-induced metastable condition has potentially severe implications in blockage of common rail systems. The condition is alleviated with the immediate reduction of pressure.

The expected increase in viscosity with pressure is attributed to the reduction of volume restricting movement of the long chain hydrocarbon molecules. In addition to the increase viscosity with pressure, each of the fuels was also noted as being temperature dependent with the lowering of viscosity with the increasing temperature. This phenomenon is to be expected due to the increase in molecular vibration and movement.

The ranked increase in viscosity with pressure across the temperature range was found to be Fuel 4 < Fuel 5 < Fuel 3 < Fuel 1 < Fuel 2. While it can be concluded that the viscosities increased with increasing pressure and decreased temperature, Fuel 2 which contained both handling and performance additives from Refinery 1, the viscosities were higher than those of Fuel 1 from the same refinery which did not contain the additives (Figures 2 and 4). However, Fuel 3 from another British refinery also with handling and performance additives did not feature the same viscosity effects (Figure 6). There was a marginal increase in comparative viscosities for Fuel 3 when mixed with 5% rapeseed biodiesel (Figure 8). This is perhaps to be expected since biodiesels generally feature higher pressure-induced viscosities [15]. Interestingly, the fuels from the two refineries were compared with diesel fuel obtained from the forecourt fuel of a commercial fuel retailer (Fuel 5). This fuel was most comparable to Fuel 1 without additives (Compare Figures 2 and 10).

Figure 12 illustrates the variation of the viscosities of the five fuels at 298 K for comparative purposes in which it can be seen that Fuel 2 from Refinery 1, with both handling and performance additives, has the highest viscosity over the widest range. The viscosity of the mineral Fuel 3 from Refinery 2 was found to be similar to the viscosity of the same fuel with the 5% biodiesel additive (Fuel 4).

In terms of density variation with temperature and pressure, each of the fuels illustrated an increase in density variation with increasing pressure, and decrease in density with temperature elevation (Table 4). Both phenomena are expected due to the compression of molecules and reduction of molecular vibration, respectively. However, it was also noted that Fuels 1, 2, and 3 from the two refineries, with and without additives, had very similar densities (Figures 3, 5, and 7), only marginally increasing for Fuel 3 with the biodiesel additive (Fuel 4, Figure 9). The highest density was found for the retail Fuel 5 (Figure 11). There is clearly a variability in the density of fuels with both temperature and pressure, and the influence of additives, which are added by the refineries.

Figure 12. Comparison of the viscosities at high pressure at 298 K. + Fuel 1, ♦ Fuel 2, ■ Fuel 3, X Fuel 4, and ▲ Fuel 5.

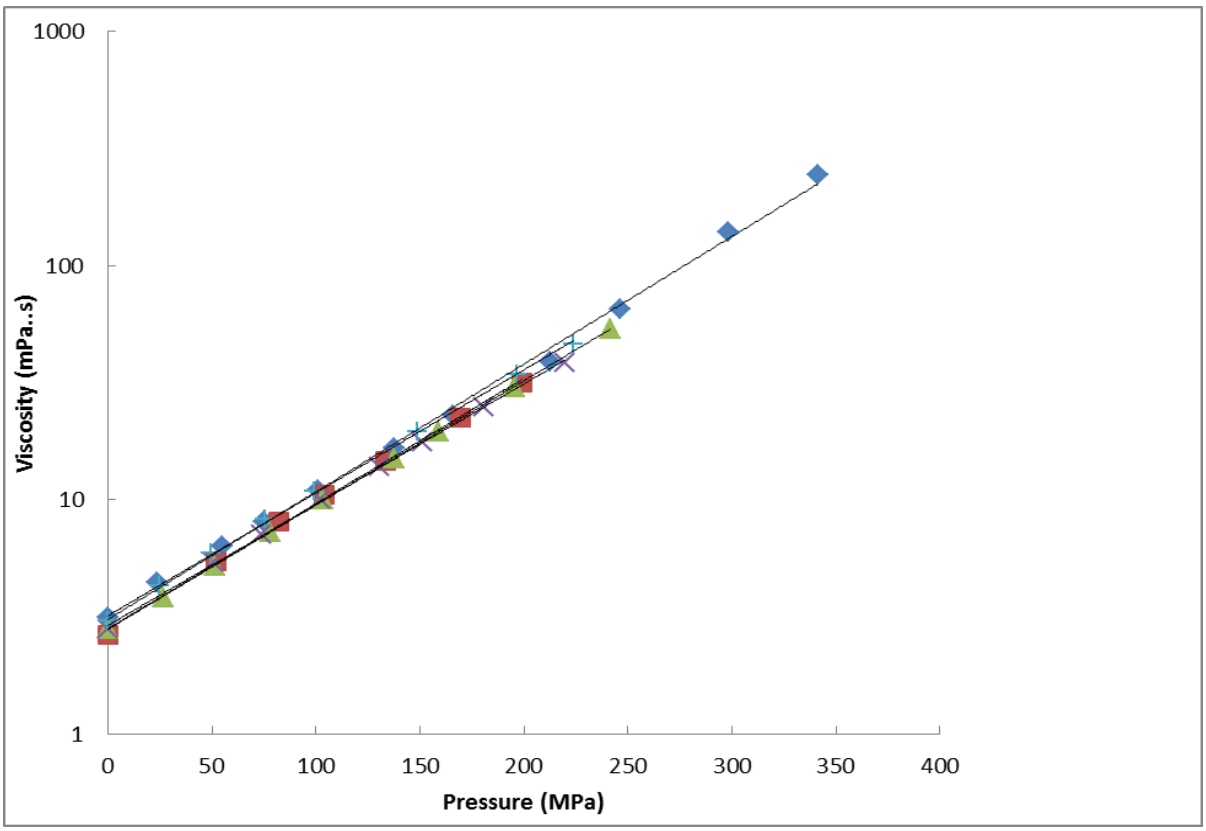

In this work, experimental data for both viscosity and density was obtained for the diesel fuels. For accurate and reliable data, it was necessary to calibrate accurately the micro-pVT and high-pressure viscometer instruments. This required the use of calibration fluids that have known temperature and pressure variations. While useful, the use of equations of state and other correlations are limited to pure liquids or the use of simple mixtures. This is therefore problematic when considering the complexity of such refinery diesel fuels. Equations such as the Tait equation are useful and reliable but

rely of the evaluation of many constants. More simple models have been developed, with some success, which require a single constant [4,5]. Certainly, the reliability and accuracy of experimental data from the high-pressure viscometer and micro-pVT instruments are imperative if the data is to be meaningful for design, operational, and fiscal purposes.

The variation of the falling-sinker viscometer coefficient A was examined with respect to the variation of the modified Reynolds number. It is noted that the thermal expansion coefficient and compressibility of the sinker are small (7.6×10^{-6}/K and 3.075×10^{-6}/MPa, respectively) and can thus be ignored. In contrast, small measurement errors in radii of the tube and sinker, r_1 and r_2, result in significant errors; the effects of which have been studied by Wehbeh *et al.* [16]. Ideally, the coefficient A is based on the physical dimensions of the sinker as shown. In practice, however, there is often a deviation in viscosity determined experimentally due to wall and end effects [17–20]. The coefficient A is therefore adjusted using a calibration liquid of known properties under high pressure [21]. To confirm the cause of these deviations, 2-D and 3-D CFD studies have previously shown the presence of vortices shedding from the trailing edge of the sinker. The simulations have shown that fully developed laminar flow is not met within the annular gap [22,23]. It has, however, been confirmed that the coefficient A tends towards the theoretical value for modified Reynolds numbers below 60.

An incidental feature of the high-pressure viscometer is the detection of phase change in mixtures. This was highlighted by measurements made using diesel fuel with no additives at 298 K (Figure 12). A phase change of the heavier components prevents the movements of the sinker in the tube. In the fuel injector of the common rail diesel engine, the phenomenon of phase change is, however, unlikely to be a cause for concern in normal operation as the temperature of the engine will be higher than those used in the laboratory and the processes too fast for thermodynamic equilibrium to be obtained. However, from a thermodynamic viewpoint, these measurements provide useful information on the nature of freezing in mixtures and their detection. They also confirm reported problems of power loss and poor engine performance in cold start situations, where the fuel temperature entering the injector may be low enough to allow partial freezing and, hence. incomplete combustion.

4. Conclusions

The viscosity data for five diesel fuels was found by measurement of the terminal sinker fall times at pressures up to 500 MPa for temperatures up to 373 K. The viscosities of each of the fuels were found to increase exponentially with both increasing pressure and increasing temperature. This relationship is confirmed with the logarithmic plot of viscosity with pressure shown in Figure 12. The accuracy of the data is dependent on sound experimental set up and requires the careful selection of a self-centering sinker and need for its calibration prior to testing. With the need for thermal stability for the equipment and long sinker descent times and subsequent restart by returning the sinker back down the tube by inverting the pressure vessel, this is a lengthy and time consuming process. The viscosity evaluations were also dependent on good density data with pressure. In this case, the equations of state, the Tait equation and experimental data using a micro-PVT apparatus provided the necessary data. The demand for accurate liquid data with pressure and temperature is essential if such data is to be of value and successfully used in an increasing number of high-pressure processes and applications.

Acknowledgments

The authors are grateful for the support of Stewart Vant, University of Strathclyde, and Gordon Reid, Delphi Diesel Systems in Gillingham ME8 0RU.

Conflict of Interest

The authors declare no conflict of interest.

References

1. Lee, S.W.; Tanaka, D.; Kusaka, J.; Daisho, Y. Effects of diesel fuel characteristics on spray and combustion in a diesel engine. *JSAE Rev.* **2002**, *23*, 407–414.
2. Yamaki, Y.; Mori, K.; Kohketsu, S.; Mori, K.; Kato, T. *Heavy Duty Diesel Engine with Common Rail Type Fuel Injection Systems*. Japanese Society of Automotive Engineers: Tokyo, Japan, 1995.
3. Riazi, M.R.; Al-Otaibi, G.N. Estimation of viscosity of liquid hydrocarbon systems. *Fuel* **2001**, *80*, 27–32.
4. Duncan, A.M.; Noorbahiyah, P.; Depcik, C.D.; Scurto, A.M.; Stagg-Williams, S.M. High-pressure viscosity of soybean-oil-based biodiesel blends with ultra-low sulfur diesel fuel. *Energy Fuels* **2012**, *26*, 7023–7036.
5. Duncan, A.M.; Ahosseini, A.; McHenry, R.; Depcik, C.D.; Stagg-Williams, S.M.; Scurto, A.M. High-pressure viscosity of biodiesel from Soybean, Canola, and Canola Oils. *Energy Fuels* **2010**, *24*, 5708–5716.
6. Park, N.A.; Irvine, T.F. The falling needle viscometer—A new technique for viscosity measurements. *Warme Stoffubertrag* **1984**, *18*, 201–206.
7. Harris, K.R.; Kanakubo, M.; Woolf, L.A. Temperature and pressure dependence of the viscosity of the ionic liquids 1-hexyl-3-methylimidazolium hexafluorophosphate and 1-butyl-3-methylimidazolium bis(trifluoromethylsulfonyl)imide. *J. Chem. Eng. Data* **2007**, *52*, 1080–1085.
8. Davis, A.M.J.; Brenner, H. The falling-needle viscometer. *Phys. Fluids* **2001**, *13*, 3086–3088.
9. Isdale, J. Viscosity of Simple Liquids including Measurement and Prediction at Elevated Pressure. Ph.D. Thesis, University of Strathclyde, Glasgow, UK, 1976.
10. Kumagai, A.; Kawase, Y.; Yokoyama, C. Falling capillary tube viscometer suitable for liquids at high pressure. *Rev. Sci. Instrum.* **1998**, *69*, 1441–1445.
11. Vant, S.C. Investigation of Fluid Properties at Non-Ambient Conditions. Ph.D. Thesis, University of Strathclyde, Glasgow, UK, 2002.
12. Dymond, J.H.; Isdale, J.D.; Glen, N.F. Density-measurement at high-pressure. *Fluid Phase Equilib.* **1985**, *20*, 305–314.
13. Belonenko, V.N.; Troitsky, V.M.; Belyaev, Y.E.; Dymond, J.H.; Glen, N.F. Application of a micro-(p, V, T) apparatus for measurement of liquid densities at pressures up to 500 MPa. *J. Chem. Thermodyn.* **2000**, *32*, 1203–1219.

14. Lee, B.I.; Kesler, M.G. Generalized thermodynamic correlation based on 3-parameter corresponding states. *AIChE J.* **1975**, *21*, 510–527.
15. Paton, J.M.; Schaschke, C.J. Viscosity measurement of biodiesel at high pressure with a falling sinker viscometer. *Chem. Eng. Res. Des.* **2009**, *87*, 1520–1526.
16. Wehbeh, E.G.; Ui, T.J.; Hussey, R.G. End effects for the falling cylinder viscometer. *Phys. Fluids A* **1993**, *5*, 25–33.
17. Huang, P.Y.; Feng, J. Wall effects on the flow of viscoelastic fluids around a circular-cylinder. *J. Non-Newton. Fluid* **1995**, *60*, 179–198.
18. Lommatzsch, T.; Megharfi, M.; Mahe, E.; Devin, E. Conceptual study of an absolute falling-ball viscometer. *Metrologia* **2001**, *38*, 531–534.
19. Stalnaker, J.F.; Hussey, R.G. Wall effects on cylinder drag at low reynolds-number. *Phys. Fluids* **1979**, *22*, 603–613.
20. Ristow, G.H. Wall correction factor for sinking cylinders in fluids. *Phys. Rev. E* **1997**, *55*, 2808–2813.
21. Park, N.A.; Irvine, T.F. Falling cylinder viscometer end correction factor. *Rev. Sci. Instrum.* **1995**, *66*, 3982–3984.
22. Schaschke, C.J.; Abid, S.; Fletcher, I.; Heslop, M.J. Evaluation of a falling sinker-type viscometer at high pressure using edible oil. *J. Food Eng.* **2008**, *87*, 51–58.
23. Gui, F.L.; Irvine, T.F. Theoretical and experimental-study of the falling cylinder viscometer. *Int. J. Heat Mass Tran.* **1994**, *37*, 41–50.